

Properties of Coatings Manufactured from Titanium Powder

Yu. N. Tyurin^a, S. G. Polyakov^a, O. V. Kolisnichenko^a, L. I. Nyrkova^a, O. N. Ivanov^b, M. G. Kovaleva^b,
O. N. Maradudina^b, and Ya. V. Trusova

^a Paton Electric Welding Institute, National Academy of Sciences of Ukraine, Kiev, Ukraine

^b Belgorod State University, Joint Research Center Diagnostic of Structure and Properties of Nanomaterials,
Belgorod, 308034 Russia

e-mail: Kovaleva@bsu.edu.ru

Abstract—The properties of coatings manufactured from titanium powder are described in this study. Coatings with thicknesses of 100 and 200 μm were deposited on a steel substrate using cumulative-detonation technology. The investigations showed the low porosity of the coatings and the absence of defects at the boundary with the substrate. Scratch tests of the coatings fixed their high adhesion and cohesion properties. Corrosion tests showed that the protective properties of the coatings are fairly high in NaCl and low in HCL. Increasing the thickness of the coatings to 0.2 mm strengthens their protective properties. Nanodispersion compounds of titanium with iron, oxygen, and carbon that decrease the corrosion resistance of the specimens in the chlorohydric acid were detected in the coatings.

INTRODUCTION

Titanium alloys are used in aircraft engineering and, due to their high corrosion resistance, they are also used in shipbuilding to produce marine screw propellers, to plate marine and submarine vessels, etc. At present, the deposition of the coatings from titanium powder by the cold spray method, HVOF [1–4], and plasma sputtering of the wire is intensively used [5]. The obtained coatings are porous and have many defects at the boundary. The coating adhesion was in the range of 30–50 MPa. The application of nitrogen as a protection gas was noted to induce local phases with a hardness of 700–1500 HV. Those phases were found to contain up to 30 at % nitrogen and 3 at % oxygen.

This study is aimed at developing a technique for depositing coatings onto a steel substrate (0.3% C) using titanium powder and examining the mechanical and corrosion properties of the coatings.

TECHNOLOGY OF COATING DEPOSITION

A cumulative-detonation sprayer (CDS) [6] and a titanium powder with a fraction of 10–50 μm (Raymor Industries Inc. production) were used for coating deposition. The powder was supplied to the CDS with nitrogen at 0.7 m^3/h at a production velocity of 0.83 kg/h. As a combustion mixture, C_3H_8 , O_2 , and air were used at consumptions of 0.536, 2.303 and 1.466 m^3/h , correspondingly. Coatings 100 and 200 μm thick were deposited for the study.

RESULTS AND DISCUSSION

The results of the investigations showed that the coating is uniform and consists of lamellae caused by the deformation of the heated and accelerated titanium particles (Fig. 1). An analysis of the boundary of the coating with the substrate showed that the visible boundary has no defects (Figs. 1a, 1b). The hardness of the transition layer (point 2) is 1500 MPa (point 3) (Fig. 1c). An element-by-element analysis of the coating composition was performed in regions of hardness measurements (Table 1). The transition layer (point 2) contains iron (up to 13 wt %) and oxygen (up to 17 wt %) in addition to titanium.

This region was formed due to the interaction of the heated titanium, oxygen, and iron (the substrate material). The local phase and structural analysis of the cumulative-detonation coating showed that the intermediate layer between the lamellae of the deformed titanium particles consists of 30- μm titanium nanocrystallites (solid phases) free from disloca-

Table 1. Element-by-element analysis at points (Fig. 1b)

Measurement point	Ti, wt %/at %	Fe, wt %/at %	O, wt %/at %
1	99.34/99.43	0.66/0.57	—
2	69.35/53.65	13.20/8.76	17.45/37.59
3	—	100.0/100.0	—

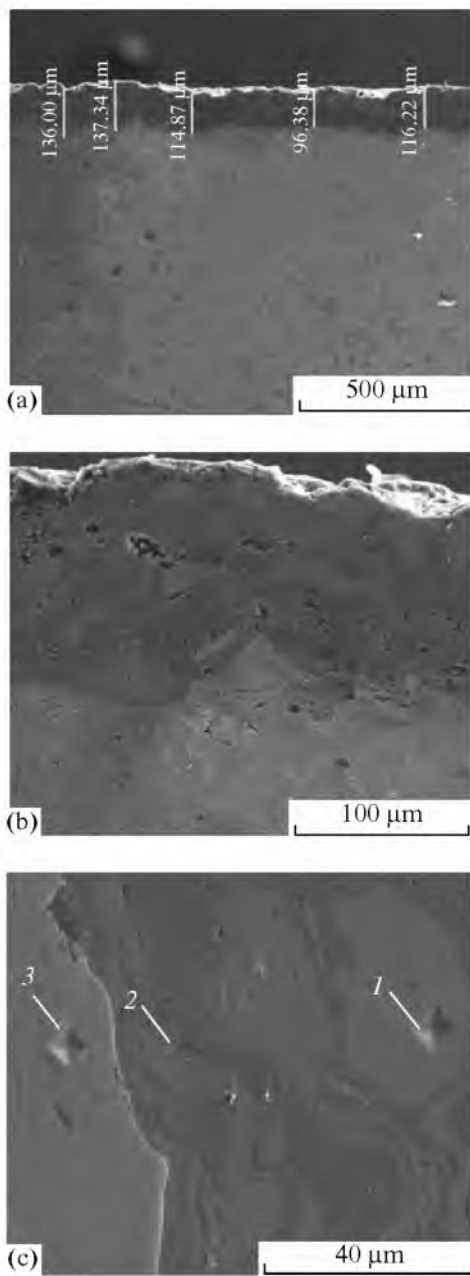


Fig. 1. Structure of coating manufactured from titanium powder: (a, b) transverse polished section of coating. (c) Marks for measuring hardness: 1—coating; 2—transition layer; 3—substrate.

tions and separated by an interlayer of the amorphous compounds of titanium with carbon and oxygen (Fig. 2a) and the crystallites of titanium oxide with a cubical lattice (Fig. 2b).

This is supported by the results of the X-ray and structural analysis of the coating (Fig. 3). The performed phase analysis shows that the main phase of the coating layer is Ti with a face-centered, closely packed lattice ($a = 2.965 \text{ \AA}$) (Fig. 3). The presence of

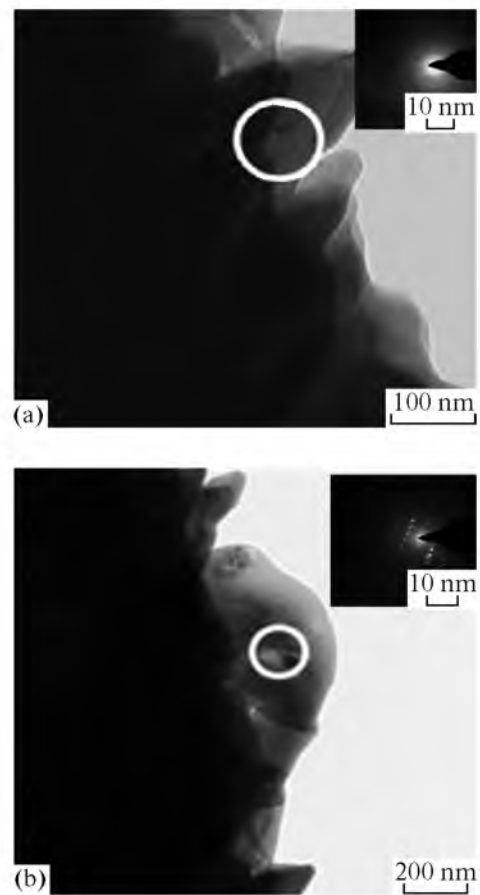


Fig. 2. Image of coating material obtained by TEM with diffraction.

other phases was indicated by the reflexes in the range of angle of $10\text{--}40^\circ$. The interplanar distances (which we managed to estimate) calculated with respect to reflexes make it possible to consider the presence of the following phases in the coating: TiC with a cubical lattice ($a = 4.349 \text{ \AA}$) and TiO with a cubical lattice ($a = 4.027 \text{ \AA}$). The complex phases in an intercrystallite space have amorphous and nanocrystalline states, which is confirmed by the results of transmission electronic microscopy. This state is accounted for by the high temperatures of material heating during the manufacturing of the coating [7].

Thus, a coating that consists of titanium and high-strength interlayers of titanium compounds is assumed to enhance the resilience and deformation resistance of the coating. The latter is supported by the results of the scratch tests of the coating using a Revetest scratch tester (CSM Instruments) (Fig. 4) [8].

The surfaces were applied scratches at a continuously increasing load in the range of $0.9\text{--}190 \text{ N}$ (Fig. 4a). A spherical diamond Rockwell C-type indenter was used with a rounding radius of $200 \text{ }\mu\text{m}$. The moment of the adhesion and cohesion destruc-

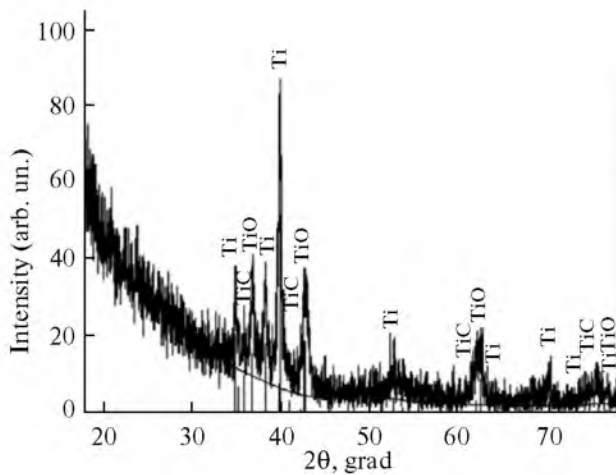


Fig. 3. Section of coating diffractogram.

tion of the coating was fixed using an optical microscope equipped with a digital camera, as well as according to the modification of the acoustic emission, the coefficient of friction, and the depth of the indenter penetration. In addition, to determine the character of the destruction, after the tests, the microstructure of the coating layer was studied using a Quanta 200 3D (Fig. 4b) raster electron-ion microscope.

Conventionally, the process destroying the coating by scratching it with an indenter can be divided into four stages. In the range of 0.9–19.8 N, the monotonous penetration of the indenter into the coating occurs; the coefficient of treatment slightly increases and the signal of the acoustic emission remains unchanged. At a load of 19.81, the indenter is found to be completely immersed in the coating. The coefficient of friction while the diamond indenter is sliding across the coating is 0.45. An increase in the load (67.07–95.57 N) involves squeezing out the material in front of the indenter in the form of small bulges and an increase in the depth of penetration of the indenter are observed (stage I).

Overcoming the bulges by an indenter is accompanied by the growth of the coefficient of friction and is marked by peaks of acoustic emissions. At loads of 95.57–120.76 N (stage II), a sharp increase in the depth of penetration of the indenter and the coefficient of friction was registered that correlates with the coating material being forced aside and its tightening on the substrate surface. Increasing the load above 120.76 N (stage III) leads to the abrupt growth of the coefficient of friction with the coating material being squeezed out and the appearance of the first cracks at the bottom of the scratch (which is marked by the peaks of the acoustic emission).

With an increase in the load, the coating is pressed into the material of the substrate (stage IV) accompanied by the formation of multiple transversal cracks at the bottom of the scratch and the intense cohesion destruction of the material of the titanium coating (Fig. 4b). An analysis of the results of the study shows that the jumps with respect to the depth of the indenter penetration, the coefficient of friction, and the acoustic emissions that are typical of the loss of the adhesion connection of the coating–substrate system were not fixed. Furthermore, after a load of 133 N, a decrease in the coefficient of friction is detected and the indenter pressing into the coating almost stops. The deformed coating has cracks, but lacks shears and destructions (Fig. 4b). Elemental analysis at the bottom of the groove left by the indenter showed the absence of Fe at point 1, but up to 4 wt % Fe and 22 wt % O were observed at point 2. This is indicative of the thinning and partial destruction of the coating at the bottom of the groove almost as deep as the transition layer (point 2) (Fig. 4b).

The next stage in defining the qualitative characteristics of the coating were the corrosion-mechanical tests [9]. The qualitative estimation of the adhesion strength of the coating with the basic metal (adhesion) according to the GOST 9.304–87 showed that the adhesion corresponds to a maximum force of 1. The absorption of moisture was 0.90 mg/cm² (GOST 4650–80, method A), which corresponds to a porosity below 1%. The electrochemical characteristics of the titanium coating and the layer (without a steel substrate) were determined by measuring the potential and the velocity of corrosion in the solution of 3% NaCl and 3% HCl with respect to a silver-chloride comparison electrode. Figure 5 shows the obtained results.

The investigations showed that, in 3% NaCl solution, in the course of the experiment, the potential of the titanium coatings shifts to the region of more negative values from 0.18 V (the thickness of the coating is 100 μm) and 0.08 V (the thickness is 200 μm) to –0.45 and 0.47 V, correspondingly, and stabilizes close to the value that is more positive than the steel potential by 0.2 V. The potential of a titanium coating without the substrate changes slightly in the course of the experiment and becomes steady close to the value of 0.2 V, which is more positive than the steel potential by about 0.8 V (Fig. 5a).

In 3% HCl solution, the following behavior is observed. At the initial moment of time, the potential of a 100-μm-thick coating is –0.07 V and it shifts to the region of more negative values up to –0.52 V and, in the case of a 200 μm-thick coating, it shifts from –0.39 to –0.5 V. The corrosion potential of steel St. 3 is –0.47 V (Fig. 5b) in this solution.

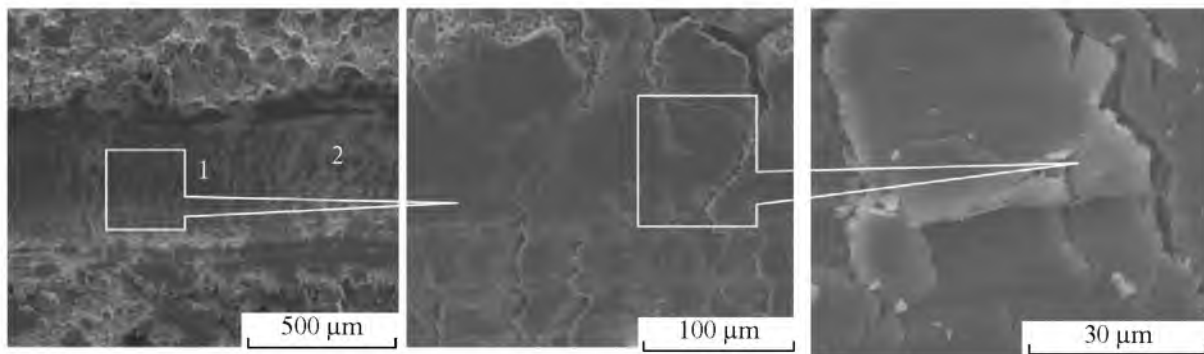
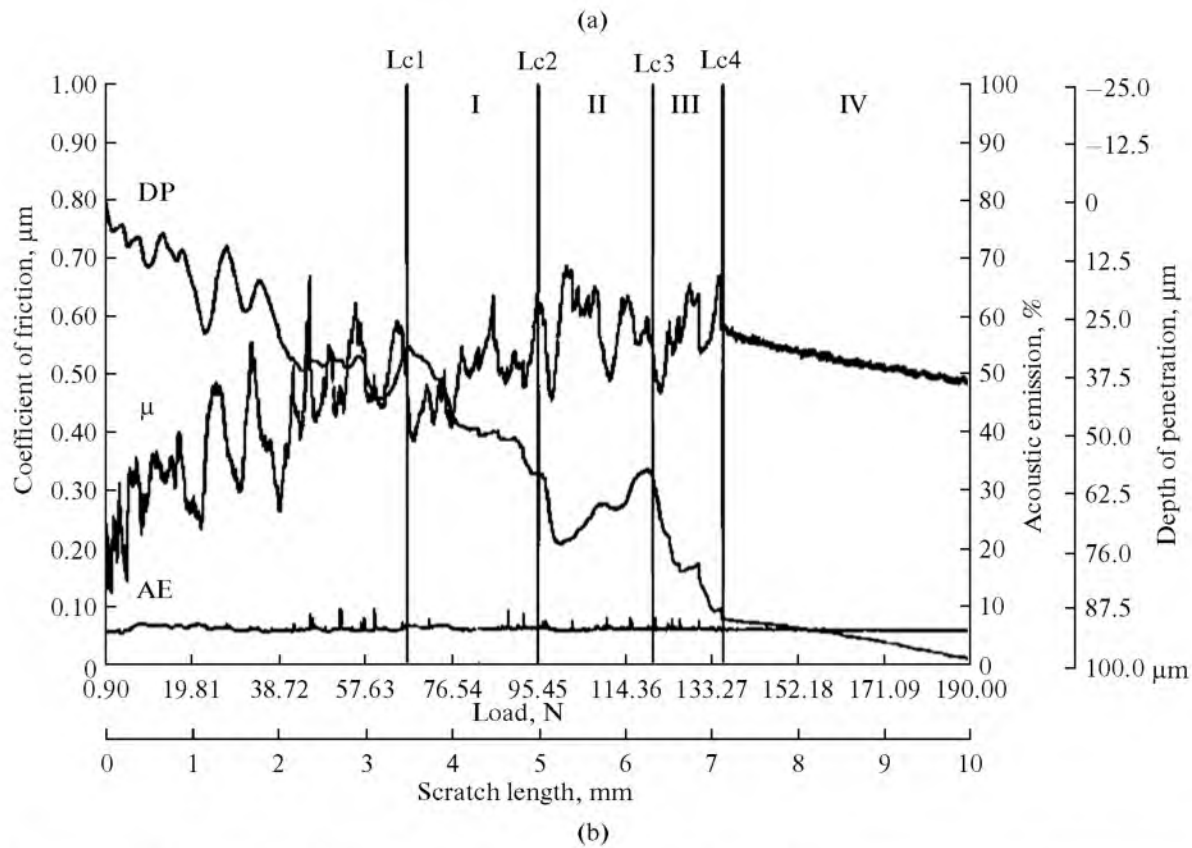


Fig. 4. Results of scratch testing with Revetest indenter (CSM Instruments): (a) acoustic emission (AE), coefficient of friction μ and depth of indenter penetration (h); (b) image of contact zone of surface with diamond indenter at load of 200 N.

The obtained experimental data show that, in 3% NaCl medium, the protective properties of the titanium coating are weaker than those of the coating material itself. In 3% HCl medium, the potential of the corrosion of the coating material approaches the steel potential. The corrosion velocity in the titanium coating was determined in 3% NaCl and 3% HCl solutions using the method of polarization resistance at UISK-101 corrosimeter (Fig. 6). In the 3% NaCl solution, the corrosion velocity of the titanium coating was found to be higher than that of steel, regardless of

the coating thickness; in the 3% HCl solution, the velocity of the corrosion of the titanium coating also exceeded that of steel.

It should also be noted that the corrosion velocity of the coating initially exceeds that of steel; however, over time, it decreases and becomes less than the corrosion velocity of steel in both solutions. This can apparently be accounted for by the activity of the titanium binding with the elements of the working gases (oxygen, carbon and metals), which primarily dissolve

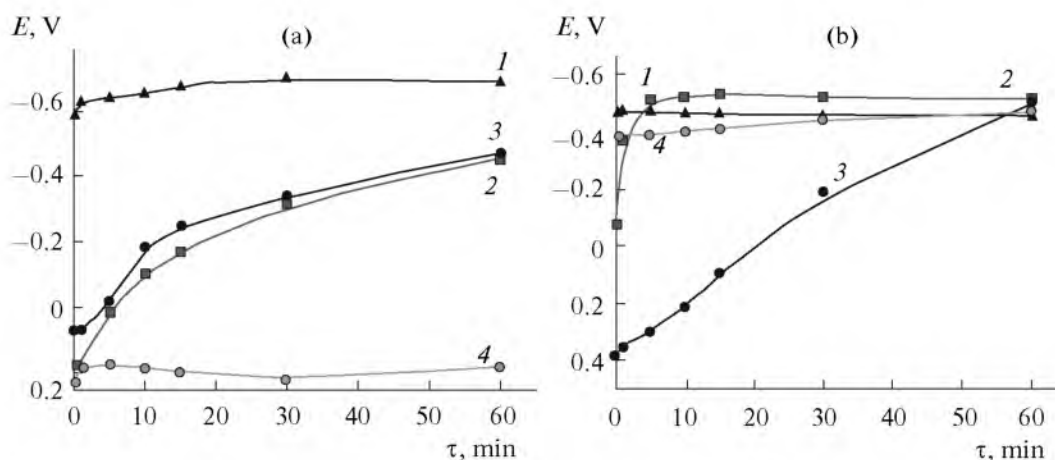


Fig. 5. Dynamics of change in corrosion potential of titanium coating with different thickness and steel St. 3 in 3% NaCl and 5% HCl solutions (b): 1—steel (0.3%); 2—200- μm -thick coating; 3—100- μm -thick coating; 4—coating without substrate.

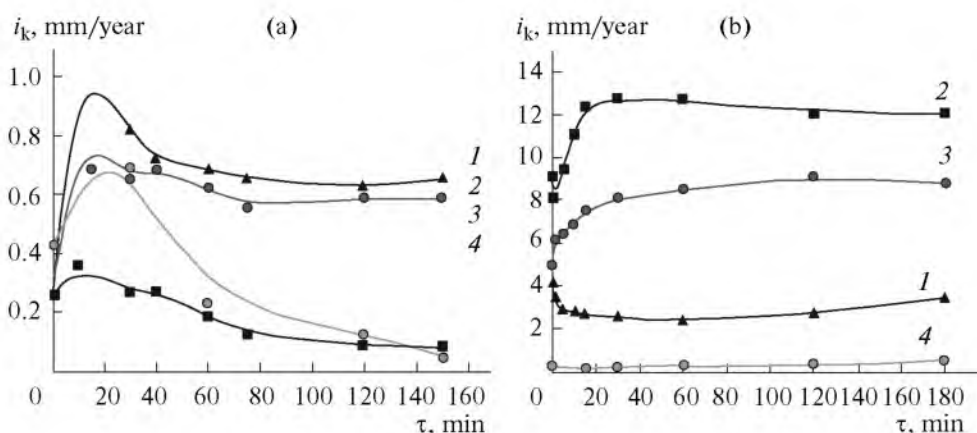


Fig. 6. Corrosion of coating and steel St. 3 in solutions: (a) 3% NaCl; (b) 3% HCl. 1—steel (0.3% C); 2—200- μm -thick coating; 3—100- μm -thick coating; 4—coating without substrate.

in the pores and on the coating surface, after which the corrosion velocity decreases.

The increase in the corrosion velocity of the titanium coating on the substrate can be correlated with the dilution of the nanodisperse compounds of titanium with iron, carbon, and oxygen (which are highly reactive) at the coating–substrate boundary.

The corrosion velocity of the coating in the 3% NaCl and 3% HCl solutions was simultaneously determined using the mass-metric method and the polarization resistance method. The obtained results are listed in Table 2. An analysis of the experimental results shows that, in 3% HCl solution, the coating is completely separated from the surface of the metal substrate. The compounds of titanium and iron are known to be highly soluble in hydrochloric acid. The presence of the iron and titanium compounds at the

boundary layer is confirmed by an element-by-element analysis (Table 1).

The coating's resistance to dilution is fairly high in 3% HCl solution (<1 mm/year); it also rather rapidly stabilizes its solubility in 3% NaCl solution (<0.1 mm/year) (Fig. 6).

Taking into account that all specimens were 0.1 and 0.2 μm thick with a value of moisture absorption of 0.90 mg/cm², their corrosion was also induced by the penetration of the active solutions through the coating to the substrate. This is confirmed by the increase in the coating thickness from 0.1 mm to 0.2 mm, which decreases the corrosion velocity in 3% NaCl solution. The substrate material (steel) in 3% HCl and 3% NaCl solutions exhibits lower corrosive resistance than the coating material that separated from the specimen (Table 2).

Table 2. Physicochemical and electrochemical characteristics of gas-thermal titanium coating and steel

Medium	Steel	Coating thickness on the substrate		Coating without the substrate
		100 μm	200 μm	
Corrosion velocity. Method of polarization resistance, vv/year				
3% NaCl	0.085	0.587	0.652	0.05
3% HCl	3.4	12.07	8.81	0.5
Corrosion velocity. Mass-metric method, mm/year				
3% NaCl;	0.18	0.0055	–	–
3% HCl	10.0	Coating has separated	–	–
Corrosion potential after 1 h				
3% NaCl;	–0.685	–0.451	–0.467	0.182
3% HCl	–0.467	–0.521	–0.499	–0.469

CONCLUSIONS

The cumulative-detonation technology makes it possible to apply high quality titanium coatings on the steel substrate. The coating consists of the deformed titanium particles with the intermediate layers of the titanium oxide and carbide with a nanocrystalline structure. This coating is thin, dense and with a good substrate adhesion. The corrosive resistance of the coating in HCl (3%) is low, which results from the solubility of the nanodisperse compounds of titanium with iron, oxygen, and carbon and a porosity of up to 1%. The corrosive resistance of the coating in NaCl is fairly high. One variant of increasing the corrosive resistance of the coating is the decrease of its oxidation, an increase in the thickness of the coating to 0.3–0.4 mm, and closing the pores by their impregnation.

ACKNOWLEDGMENTS

This study is performed using the equipment of the Belgorod State University Joint Research Center Diagnostic of Structure and Properties of Nanomaterials in the framework of a State Contract of the Federal Target Program no. 02.552.11.7066.

REFERENCES

1. Blose, R.E., *Proc. Int. Thermal Spray Conf. "ITSC 2005"*, Switzerland, Basel, 2005, P.199.
2. Jin Kawakita and Seiji Kuroda, Takeshi Fukushima et al., *Surf. Coatings Technol.*, 2006, no. 201, P.1250.
3. Kim K.H., Watanabe M., Mitsuishi K. et al., *Proc. Int. Thermal Spray Conf. "ITSC 2008"*, Netherland, Maas-tricht, 2008, P.1277.
4. Rezaeian, A., Chromik, R.R., Yue, S. et al., *Proc. Int. Thermal Spray Conf. "ITSC 2008"*, Netherland, Maas-tricht, 2008, P.842.
5. Bach, Fr.-W., Mohwald, K., and Kolar, D., *Proc. Int. Thermal Spray Conf. "TSC 2005"*, Switzerland, Basel, 2005, p.1199.
6. Tyurin, Yu.N., Kolisnichenko, O.V., and Duda, I.M., *Strength. Technol. Coat.*, 2009, no. 5, p. 27.
7. Levashov, E.A. and Shtanskii, D.V., *Usp. Khim.*, 2007, vol. 76, no. 5, p. 501.
8. Hintermann, H.E., *Fresenius J. Anal. Chem., ser. B*, 1993, vol. 346, p. 45.
9. Chviruk, V.P., Polyakov, S.G., and Gerasimenko, Yu.S., *Elektrokhimichnii monitoring tekhnogennikh seredov-ishch (Electrochemical Monitoring of Technogenic Media*, Kiev: Akadempriodika, 2007, p. 384.